This is a preprint, the final version is subject to change, of the American Mineralogist (MSA)
Cite as Authors (Year) Title. American Mineralogist, in press.
(DOI will not work until issue is live.) DOI: http://dx.doi.org/10.2138/am.2014.4434

Revision 1

Influence of H_2 fluid on the stability and dissolution of Mg_2SiO_4 forsterite under high pressure and high temperature

Ayako Shinozaki[1*], Hisako Hirai[1], Hiroaki Ohfuji[1], Taku Okada[2], Shin-ichi Machida[1†] and Takehiko Yagi[2††]

[1]Geodynamics Research Center, Ehime University, 2-5 Bunkyo-cho, Matsuyama, Ehime, 790-8577, Japan

[2]Institute for Solid State Physics, The University of Tokyo, Kashiwanoha, Kashiwa, Chiba 277-8581, Japan

[*]Present address: Geochemical Research Center, Graduate School of Science, The University of Tokyo, Hongo, Tokyo 113-0033, Japan

[†]Present address: Geophysical Laboratory, Carnegie Institution of Washington, 5251 Broad Branch Rd. N.W. Washington, DC 20015, USA

[††]Present address: Geodynamics Research Center, Ehime University, 2-5 Bunkyo-cho, Matsuyama, Ehime, 790-8577, Japan

This is a preprint, the final version is subject to change, of the American Mineralogist (MSA)
Cite as Authors (Year) Title. American Mineralogist, in press.
(DOI will not work until issue is live.) DOI: http://dx.doi.org/10.2138/am.2014.4434

Abstract

High pressure and high temperature experiments were carried out in a Mg_2SiO_4-H_2 system using laser-heated diamond anvil cells to understand the influence of H_2 fluid on the stability of forsterite. *In situ* X-ray diffraction experiments and Raman spectroscopic measurements showed the decomposition of forsterite, and formation of periclase (MgO) and stishovite/quartz (SiO_2) in the presence of H_2 after being heated in the range between 2.5 GPa, 1400 K and 15.0 GPa, 1500 K. Transmission electron microscopic observation of the samples recovered from 15.0 GPa and 1500 K showed that the granular to columnar periclase grains maintained the original grain shape of forsterite, indicating that the periclase crystals crystallized under high temperature. On the other hand, euhedral columnar stishovite crystals were found at the boundaries between residual forsterite grains and reacted periclase. This implies that the SiO_2 component was dissolved in H_2 fluid, and that stishovite was considered to have crystallized when the solubility of the SiO_2 component became reduced with decreasing temperature. Additional experiment on a SiO_2-H_2 system clearly showed the dissolution of quartz in H_2 fluid, while those on a MgO-H_2 system, periclase was hardly dissolved. These lines of evidence indicate that forsterite was incongruently dissolved in H_2 fluid to form periclase crystals in the Mg_2SiO_4-H_2 system which is different from what was

observed in the Mg_2SiO_4-H_2O system. The results indicate that the stability of forsterite is strongly affected by the composition of coexisting C-O-H fluid.

Keywords: H_2 fluid, forsterite, X-ray diffraction, transmission electron microscope, laser-heated diamond anvil cells

Introduction

Fluids have been known to affect the physical and chemical properties of rocks and minerals in the Earth's mantle (e.g. Taylor and Green, 1988; Litasov, 2011). For example, the presence of H_2O fluid significantly lowers the melting temperature and changes the stability fields (phase transition boundaries) of major mantle minerals (Angel et al., 2001; Litasov and Ohtani, 2003). The stability of olivine, which is the most abundant mineral in the upper mantle, is also largely influenced by coexisting H_2O fluid. For example, the melting temperature decreases to about 1200 K at 10 GPa in the presence of H_2O fluid (Inoue, 1994), and the phase transition pressure to wadsleyite is also lowered by about 1 GPa at 1473 K and by about 0.4 GPa at 1673 K compared with the anhydrous condition (Frost and Dolejs, 2007). The stability of forsterite depends on the solubility of Si and Mg components in coexisting H_2O fluid. (Nakamura and Kushiro, 1974; Ryabchikov et al., 1982; Zhang and Frantz, 2000; Mibe et al., 2002; Kawamoto et al., 2004). Nakamura and Kushiro (1974) first found that the SiO_2 content in H_2O fluid coexisting with forsterite reaches ~20 wt% at 1.5 GPa and around 1550 K. The solubility of SiO_2 increases with pressure below 3 GPa, while above this pressure, MgO becomes more soluble (Inoue, 1994; Stalder et al., 2001; Mibe et al., 2002; Kawamoto et al., 2004). Forsterite is a thermodynamically stable phase coexisting with

60 H_2O fluid alone up to around 9 GPa in the Mg_2SiO_4-H_2O system, while above this
61 pressure clinoenstatite ($MgSiO_3$) is stable (Inoue, 1994).

62 In the Earth's mantle, fluids are supposed to be present not only as H_2O but
63 also as mixtures with other components such as CO_2, CH_4, and H_2. The chemical
64 composition of such C-O-H fluids depends largely on the oxidation state of the
65 surrounding mantle (Taylor and Green, 1988; Ballhaus and Frost, 1994; Ballhaus, 1995;
66 Frost and McCammon, 2008). According to recent chemical analyses of mantle
67 xenoliths (O'Neill, 2001; Woodland and Koch, 2003; McCammon and Kopylova, 2004;
68 Lazarov et al., 2009), thermodynamic calculations (Ballhaus, 1995), and high pressure
69 and temperature experiments (Frost et al., 2004; Rohrbach et al., 2007; Rohrbach et al.,
70 2011), the mantle is expected to become progressively reduced with depth. At depths
71 greater than 250 km, H_2 and CH_4, in addition to H_2O, are dominant components of
72 C-O-H fluids (Ballhaus, 1995; Frost and McCammon, 2008). A recent experimental
73 study demonstrated that H_2 is likely the most dominant component in a reduced
74 condition (Mo-MoO_2 buffer) at 6.3 GPa, 1673-1873 K (Sokol et al., 2009). In addition,
75 H_2 fluids were found in some natural diamonds (Melton and Giardini 1974). These
76 studies indicate that H_2 is one of the major components of the C-O-H fluids as well as
77 H_2O and CH_4 in the deeper part of the mantle.

The effect of such reducing C-O-H fluids on the stability and physical and chemical properties of coexisting mantle minerals was also investigated using experimental approaches. Sokol et al. (2010) conducted a high pressure–temperature experiment in a system between forsterite and H_2O–CH_4–H_2 fluid at 6.3 GPa and reported that hydrous forsterite was stable at least up to 1973 K under the reduced conditions where the fluid contains 52 mol% of H_2, 30 mol% of H_2O and 12 mol% of CH_4 (Sokol et al., 2010). Recently, we performed high pressure and temperature experiments in a Mg_2SiO_4-H_2 system under 9.8-13.2 GPa and below 1000 K and found that forsterite is likely to be stable without dissolution, although the unit cell volume of forsterite coexisting with the H_2 fluid was found to be slightly larger than that of pure (dry) forsterite (Shinozaki et al., 2012). To understand the effect of H_2 fluid on stability of forsterite in the ambient mantle condition, further experiments at higher temperature is necessary. In this study, high pressure and temperature experiments in Mg_2SiO_4-H_2 system were performed, showing a remarkable influence of H_2 fluid on the stability of forsterite and showing dissolution of SiO_2 components in H_2 fluid. In addition, experiments in SiO_2-H_2 system and MgO-H_2 system were conduced to compare solubility of Si and Mg in H_2 fluid under high pressure and temperature.

Experimental

High pressure and temperature experiments were performed using a lever-and-spring type diamond anvil cell (DAC) with flat-top diamond anvils with 450 μm and 600 μm culets. Tungsten or rhenium was used as gaskets, so that H_2 fluid can be sealed properly in the sample chamber even at elevated temperature. The diameter and the initial thickness of the sample chamber were approximately 1/2 to 1/3 of the culet size and about 70 μm to 150 μm, respectively. The starting materials used in the present study of the Mg_2SiO_4-H_2 system were powdered synthetic forsterite (Mg_2SiO_4) and hydrogen gas (99.99999%). Powdered forsterite was loaded in the sample chamber together with ruby and gold particles. In the experiments in SiO_2-H_2 and MgO-H_2 systems, natural quartz (SiO_2) and synthetic periclase (MgO) were used as solid starting materials, respectively. A few particles of quartz or periclase were polished to a thickness of about 50 μm from both sides and then loaded into a sample chamber. H_2 gas was introduced using a gas-loading apparatus (Yagi et al., 1996); hydrogen gas was compressed to a supercritical fluid at approximately 0.11 to 0.15 GPa at room temperature. Pressure was measured by the ruby fluorescence method (Mao et al., 1978). In run no. 1, 2, and 4 (Table 1), the P-V-T equation of the state of gold (powder), which was mixed in the sample also as a laser absorbent, was also used to estimate pressure (Tsuchiya, 2003).

In total, five experiments were performed in the Mg_2SiO_4-H_2 system in the present study (Table 1). Two sets of additional experiments were also conducted in SiO_2-H_2 and MgO-H_2 systems (Table 1). The sample was first compressed to the target pressure at room temperature and then heated using a multi-mode neodymium-doped yttrium aluminum garnet (Nd:YAG) laser (double-side heating) or using a CO_2 laser (single-side heating). Temperature was measured by the spectroradiometric method. The uncertainly of the heating temperature was estimated to be ± 200 K from the lateral temperature distribution in the sample chamber and the fluctuation of laser power.

The samples under high pressures were characterized by *in-situ* synchrotron X-ray diffraction (XRD) and Raman spectroscopy. The high pressure and high temperature XRD measurements in run no. 1 and 2 were performed with a monochromatic X-ray beam (λ=0.4140 Å), which was collimated to 15 μm in diameter at BL10XU of Spring-8. XRD observations in run no. 3, 4, and 5 were measured using a monochromatic X-ray (λ=0.6166 Å) at BL18-C of the Photon Factory of the High Energy Accelerator Research Organization (KEK) at room temperature after heating by using a CO_2 laser. Raman spectroscopic measurements of the samples under high pressure and room temperature were performed using a diode laser (λ=473 nm) or an Ar^+ laser (λ=514.5 nm) combined with CCD-detectors with a resolution of ±2 cm^{-1}

(PHOTON Design). Samples recovered from experiments were coated with a thin gold layer, and then were analyzed using a scanning electron microscope (SEM, JSM-7000F) equipped with an energy dispersive X-ray spectrometer (EDS). For TEM observation, thin foils were prepared from selected samples using a focused ion beam (FIB) milling system (JEOL JEM-9310). The microtexture and chemical composition of the recovered samples (run no. 2, 4) were analyzed using a TEM (JEOL JEM-2010) equipped with an EDS.

Results and Discussion

We first investigated the influence of molecular hydrogen on the stability of forsterite and the potential reaction between them under high pressure and high temperature through *in-situ* XRD observations. Figure 1 shows representative XRD patterns of run no. 2 (at ~ 11 GPa) collected at room temperature before, during and after YAG laser heating at 1500 and 2200 K. Before heating, the observed diffraction peaks were all indexed with forsterite and gold (Fig. 1A). Upon heating, no change was detected in the diffraction profile below 1500 K (Fig. 1B), but when laser power was further increased to ~37 W, an abrupt increase in emission intensity (strong flashing) occurred and the temperature increased rapidly to 2500 K or even higher. Thus, we decreased the laser power quickly so that the heating temperature was stabilized at

around ~2200 K. The diffraction pattern collected during heating at 2200 K showed that the intensities of forsterite peaks decreased, while periclase (MgO) and stishovite (SiO_2) peaks newly appeared, suggesting the decomposition of forsterite (Fig. 1C). In addition, weak wadsleyite peaks were also observed. The samples were then quenched by turning off the laser power. The diffraction pattern measured after heating indicates that the major quenched phases are periclase and stishovite with small amounts of forsterite and wadsleyite (Fig. 1D). The observed abrupt jump of heating temperature (i.e. emission intensity) might be attributed to the melting of gold which was used as a laser absorbent as well as a pressure marker, since the temperature at which the emission drastically increased is close to its predicted melting point at the pressure (Tsuchiya, 2003). The formation of wadsleyite is likely limited to the low temperature regions (around the laser-heated spot), showing that the forsterite-wadsleyite transition is thermodynamically favorable even in the presence of H_2 fluid when the heating temperature does not exceed the threshold temperature for the decomposition.

To confirm whether the observed decomposition of Mg_2SiO_4 forsterite to MgO and SiO_2 in the presence of H_2 is indeed essential and reproducible, we further conducted heating experiments at around 11 GPa and 15 GPa (runs no. 3 and 4, respectively) using a CO_2 laser, which allows us to heat non-iron-bearing samples

directly and stably without using a laser absorbent. The sample was heated to around 1500-1600 K for about 20 minutes, and was analyzed by XRD after quenching to room temperature. The diffraction patterns obtained from both runs heated at ~11 GPa and ~15 GPa, (runs no. 3 and 4) showed distinct peaks of periclase and stishovite together with some peaks from the unreacted, residual forsterite, suggesting that the decomposition of forsterite likely initiates at around 1600 K at 10 GPa and at 1500 K at 15 GPa.

In order to observe the behavior of H_2 and its physical and chemical state during the runs, samples were also analyzed by Raman spectroscopy before and after heating. The H-H vibration mode was observed at around >4230 cm^{-1} both before and after heating (Fig. 2), indicating that the decomposition of forsterite into periclase and stishovite/quartz indeed occurred in the coexistence of H_2 fluid. Since the studied P-T range is in the stability field of forsterite under dry condition (Presnall and Walter, 1993), the decomposition reaction observed in the present study was presumably induced by H_2 fluid. In runs no. 1, 2 and 4, in addition to the H-H mode, a peak centered at around 3000 cm^{-1}, which can be assigned to the C-H vibration mode, was also observed after heating. This peak originated from the presence of a small amount of methane which was probably produced as a result of the reaction between H_2 and the

culet surface of diamond anvils, as observed in a similar experimental system with H_2O fluid (Chou and Anderson, 2009). However, since periclase and stishovite/quartz also formed in the sample heated at ~11.0 GPa (run no. 3) where the methane C-H peak was not observed, the presence of methane is likely not a prerequisite for the decomposition of forsterite.

To understand the detailed decomposition mechanism of forsterite and the resulting phase relations under high pressure and temperature, microtextures of the quenched samples were investigated by TEM. Figure 3a shows a TEM image of the sample recovered from 15.0 GPa and 1500 K (run no. 4). The image shows a reaction front of forsterite and H_2 fluid, where the left side consists of granular to columnar fine grains, while the right side consists of larger forsterite crystals of ~1 μm (the laser-heated center is thought to be located at the far left of this image). The electron diffraction pattern obtained from the left area shows many diffraction spots scattered along the Debye rings of periclase 111, 200, 220 and also fewer scattered spots of stishovite 220 (Fig. 3b). No obvious diffractions of forsterite were observed, indicating that forsterite had completely broken down in these areas. Figure 4 is a magnified image of the reaction front showing a distinct sharp boundary between columnar periclase crystals and a host (unreacted, residual) forsterite crystal. It is interesting to note that the

formation of periclase crystals likely initiated within a forsterite grain while maintaining the original grain shape of forsterite (as a pseudomorph). Although columnar periclase crystals appear to have grown perpendicularly from the interface of the host forsterite grain (Fig. 4), there is no specific relation between the crystal lattices of the two phases. The orientation of periclase crystals is rather random, as indicated by the ring-like electron diffraction pattern (Fig. 3b). Such a textural feature of periclase crystals implies that they are a product of rapid crystal growth such as dendritic growth and the elongated shape of the crystals likely reflect the presence of sharp thermal and chemical gradients during formation. On the other hand, stishovite crystals, which usually show a euhedral columnar morphology, were found only at boundaries between residual forsterite grains and their pseudomorphs (replaced with periclase), as shown in Figure 3 and Figure 4. This means that SiO_2 components are mostly dissolved into the H_2 fluid upon heating, but then precipitated as stishovite partially in low temperature regions even during heating and crystallized completely after quenching to room temperature due to a decrease in their solubility with decreasing temperature. On the other hand, diffraction peaks of stishovite were observed by the *in-situ* measurement even during heating at around 2200 K (Fig. 1C). They might be derived from the crystals precipitated from H_2 fluid in the low-temperature region, since there seems to be a

222 significant temperature gradient along the vertical direction of the sample during
223 heating.

224 We also conducted a low-pressure (at 2.5 GPa) experiment using the same
225 starting material (forsterite + H_2) at 2.5 GPa in order to check whether the dissolution of
226 SiO_2 into H_2 is essential at high pressure and high temperature (run no. 5). The XRD
227 pattern collected from the sample heated to 1400 K and quenched to room temperature
228 indicates the decomposition of forsterite and formation of periclase and quartz, which is
229 a low-pressure polymorph of stishovite. SEM observation showed that the most of the
230 solid product remained in the sample chamber after pressure release (Fig. 5a). Fine
231 crystals of periclase and quartz were observed only at the center of the laser-heated area,
232 while unreacted forsterite grains remain in the surrounding area. Note that most of the
233 quartz grains exhibit a spherulitic texture (Fig. 5b), while periclase crystals are
234 characterized by a columnar or occasionally dendritic texture (Fig. 5c). Both quartz and
235 periclase textures suggest considerably rapid crystal growth probably under highly
236 non-equilibrium conditions.

237 To understand the crystallization process of the spherulite texture of quartz and
238 the columnar and dendritic periclase, additional experiments of SiO_2-H_2 and MgO-H_2
239 systems were conducted (Table 1). Figure 5a shows optical micrographs of the SiO-H_2

sample (run no. 6) before heating at 1.7 GPa, in which a few quartz plates (double-sided and polished) were loaded in H_2 fluid (Fig. 6a). After heating at 1700 K at 2.0 GPa, a circular feature remained at the heating spot in one of the quartz crystals (Fig. 6b). No Raman peaks of quartz were detected within this area suggesting the dissolution of SiO_2 into H_2 fluid. In fact, the SEM image of the recovered quartz sample shows many etch pits and micro-steps on the surface (Fig. 7a), which was carefully polished before the experiment. In addition, many spherulitic quartz crystals were observed (Fig. 7b). These spherulites are assumed to have crystallized rapidly from H_2 fluid upon quenching from high temperature after heating or upon pressure release which leads H_2 fluid to be released (evaporated) from the sample chamber.

We further conducted another experiment (run no. 7) at 3.2 GPa and 1700 K using an MgO-H_2 mixture as the starting material, in which we found no evidence of the dissolution of periclase even after heating, suggesting that the solubility of MgO in H_2 is far lower than that of SiO_2 at high pressure and temperature. This is consistent with the observation that in the product from the Mg_2SiO_4-H_2 experiments the formation of columnar (dendrite-like) periclase crystals is limited within the original forsterite grains, which implies that long-range atomic diffusion was not involved in their rapid crystallization process.

In the present study, forsterite always decomposed to periclase and stishovite/quartz in the presence of H_2 fluid in the pressure range from 2.5 to 15.0 GPa and up to 1600 K. Microtexture observations of the recovered samples suggest that periclase formed simultaneously with the decomposition reaction by replacing the original forsterite grains, while stishovite/quartz crystallized essentially from H_2 fluid, which was supersaturated with SiO_2, at low temperature regions. This suggests that forsterite (Mg_2SiO_4) incongruently decomposed to form periclase (MgO) crystals and SiO_2 dissolved H_2 fluid above 1400-1600 K at pressures between 2.5 GPa and 15.0 GPa. The result is remarkably different from the MgO-SiO_2-H_2O system where no decomposition of forsterite is observed at least up to 10 GPa (Inoue, 1994; Mibe et al., 2002; Kawamoto et al., 2004), and MgO-rich component was dissolved into H_2O fluid above 3 GPa (Inoue, 1994; Stalder et al., 2001; Mibe et al., 2002; Kawamoto et al., 2004). The present results suggested that the stability of forsterite was strongly influenced by the composition of the coexisting C-O-H fluid. In the lower part of the upper mantle, H_2 fluids are thought to be one of the major components of C-O-H fluids (Ballhaus, 1995; Frost and McCammon, 2008; Sokol et al., 2009). It is expected that a certain amount of H_2 can be produced by the serpentinization of olivine in the shallow mantle (Sleep et al., 2004). In such regions, mantle rocks and minerals may have a

higher MgO content than the surrounding mantle due to the dissolution of SiO_2 components into fluid.

Acknowledgments

The synchrotron radiation experiments were performed at the BL10XU of SPring-8 with the approval of the Japan Synchrotron Radiation Research Institute (JASRI) (Proposal No. 2011A1597) and BL18-C of KEK with the approval of the Photon Factory Program Advisory Committee. This study was supported by the G-COE program Deep Earth Mineralogy. A. Shinozaki was supported by a JSPS Research Fellowship for Young Scientists.

286 References

287 Angel, R.J., Frost, D.J., Ross, N.L., and Hemley, R. (2001) Stabilities and equations of
288 state of dense hydrous magnesium silicates. Physics of the Earth and Planetary
289 Interiors, 127, 181-196.

290 Ballhaus, C. (1995) Is the upper mantle metal-saturated? Earth and Planetary Science
291 Letters, 132, 75-86.

292 Ballhaus, C., and Frost, B.R. (1994) The generation of oxidized CO_2-bearing basaltic
293 melts from reduced CH_4-bearing upper mantle sources. Geochimica et
294 Cosmochimica Acta, 58, 4931-4940.

295 Chou, I., and Anderson, A.J. (2009) Diamond dissolution and the production of methane
296 and other carbon-bearing species in hydrothermal diamond-anvil cells.
297 Geochimica et Cosmochimica Acta, 73, 6360-6366.

298 Frost, D.J., and Dolejs, D. (2007) Experimental determination of the effect of H_2O on
299 the 410-km seismic discontinuity. Earth and Planetary Science Letters, 256,
300 182-195.

301 Frost, D.J., Liebske, C., Langenhorst, F., McCammon, C.A., Trønnes, R.G., and Rubie,
302 D.C. (2004) Experimental evidence for the existence of iron-rich metal in the
303 Earth's lower mantle. Nature, 428, 409-412.

304 Frost, D.J., and McCammon, C.A. (2008) The redox state of Earth's mantle. The Annual
305 Review of Earth and Planetary Science, 36, 389-420.
306 Inoue, T. (1994) Effect of water on melting phase relations and melt composition in the
307 system Mg_2SiO_4-$MgSiO_3$-H_2O up to 15 GPa. Physics of the Earth and Planetary
308 Interiors, 85, 237-263.
309 Kawamoto, T., Matsukage, K.N., Mibe, K., Isshiki, M., Nishimura, K., Ishimatsu, N.,
310 and Ono, S. (2004) Mg/Si ratios of aqueous fluids coexisting with forsterite and
311 enstatite based on the phase relations in the Mg_2SiO_4-SiO_2-H_2O system.
312 American Mineralogist, 89, 1433.
313 Lazarov, M., Woodland, A.B., and Brey, G.P. (2009) Thermal state and redox conditions
314 of the Kaapvaal mantle: A study of xenoliths from the Finsch mine, South Africa.
315 Lithos, 112, 913-923.
316 Litasov, K., and Ohtani, E. (2003) Stability of various hydrous phases in CMAS
317 pyrolite-H_2O system up to 25 GPa. Physics and Chemistry of Minerals, 30,
318 147-156.
319 Litasov, K.D. (2011) Physicochemical conditions for melting in the Earth's mantle
320 containing a C-O-H fluid (from experimental data). Russian Geology and
321 Geophysics, 52, 475-492.

322 Mao, H., Bell, P., Shaner, J.W., and Steinberg, D. (1978) Specific volume measurements
323 of Cu, Mo, Pd, and Ag and calibration of the ruby R_1 fluorescence pressure
324 gauge from 0.06 to 1 Mbar. Journal of Applied Physics, 49, 3276-3283.
325 McCammon, C., and Kopylova, M.G. (2004) A redox profile of the Slave mantle and
326 oxygen fugacity control in the cratonic mantle. Contributions to Mineralogy and
327 Petrology, 148, 55-68.
328 Nakamura, Y., and Kushiro, I., (1974) Composition of the gas phase in
329 Mg_2SiO_4-SiO_2-H_2O at 15 kbar. Year Book Carnegie Inst Wash 73, 255–258.
330 Mibe, K., Fujii, T., and Yasuda, A. (2002) Composition of aqueous fluid coexisting with
331 mantle minerals at high pressure and its bearing on the differentiation of the
332 Earth's mantle. Geochimica et Cosmochimica Acta, 66, 2273-2285.
333 Melton, C.E., Giardini, A.A., (1974) The composition and signiWcance of gas released
334 from natural diamonds from African and Brazil. American Minneralogist
335 59:775–782
336 O'Neill, H. (2001) Oxidation during metasomatism in ultramafic xenoliths from the
337 Wesselton kimberlite, South Africa: implications for the survival of diamond.
338 Contrib Mineral Petrol, 141, 287-296.
339 Presnall, D.C., and Walter, M.J. (1993) Melting of forsterite, Mg_2SiO_4, from 9.7 to 16.5

GPa. Journal of Geophysical Research, 98, 19777-19783.

Rohrbach, A., Ballhaus, C., Golla-Schindler, U., Ulmer, P., Kamenetsky, V.S., and Kuzmin, D.V. (2007) Metal saturation in the upper mantle. Nature, 449, 456-458.

Rohrbach, A., Ballhaus, C., Ulmer, P., Golla-Schindler, U., and Schönbohm, D. (2011) Experimental evidence for a reduced metal-saturated upper mantle. Journal of Petrology, 52, 717.

Ryabchikov, I., Schreyer, W., and Abraham, K. (1982) Compositions of aqueous fluids in equilibrium with pyroxenes and olivines at mantle pressures and temperatures. Contributions to Mineralogy and Petrology, 79, 80-84.

Shinozaki, A., Hirai, H., Kagi, H., Kondo, T., Okada, T., Nishio-Hamane, D., Machida, S., Irifune, T., Kikegawa, T., and Yagi, T. (2012) Reaction of forsterite with hydrogen molecules at high pressure and temperature. Physics and Chemistry of Minerals, 39, 123-129.

Sleep, N.H., Meibom, A., Fridriksson, T., Coleman, R.G., and Bird, D.K. (2004) H_2-rich fluids from serpentinization: Geochemical and biotic implications. Proceedings of the National Academy of Sciences of the United States of America, 101, 12818-12823.

358 Sokol, A.G., Palyanova, G.A., Palyanov, Y.N., Tomilenko, A.A., and Melenevsky, V.N.
359 (2009) Fluid regime and diamond formation in the reduced mantle:
360 Experimental constraints. Geochimica et Cosmochimica Acta, 73, 5820-5834.
361 Sokol, A.G., Palyanov, Y.N., Kupriyanov, I.N., Litasov, K.D., and Polovinka, M.P.
362 (2010) Effect of oxygen fugacity on the H_2O storage capacity of forsterite in the
363 carbon-saturated systems. Geochimica et Cosmochimica Acta, 74, 4793-4806.
364 Stalder, R., Ulmer, P., Thompson, A., and Günther, D. (2001) High pressure fluids in the
365 system MgO-SiO_2-H_2O under upper mantle conditions. Contributions to
366 Mineralogy and Petrology, 140, 607-618.
367 Taylor, W.R., and Green, D.H. (1988) Measurement of reduced peridotite-COH solidus
368 and implications for redox melting of the mantle. Nature, 332, 349-352.
369 Tsuchiya, T. (2003) First-principles prediction of the PVT equation of state of gold and
370 the 660-km discontinuity in Earth's mantle. Journal of Geophysical Research,
371 108, 2462.
372 Woodland, A.B., and Koch, M. (2003) Variation in oxygen fugacity with depth in the
373 upper mantle beneath the Kaapvaal craton, Southern Africa. Earth and Planetary
374 Science Letters, 214, 295-310.
375 Yagi, T., Yusa, H., and Yamakata, M. (1996) An apparatus to load gaseous materials to

the diamond-anvil cell. Review of Scientific Instruments, 67, 2981-2984.

Zhang, Y.G., and Frantz, J.D. (2000) Enstatite-forsterite-water equilibria at elevated temperatures and pressures. American Mineralogist, 85, 918.

Figure legends

Figure 1. Representative XRD patterns of a forsterite-H_2 sample (run no. 2). (A) Before heating at 11.1 GPa at room temperature, (B) during heating at 1500 K (C) during heating at 2200 K (D) after heating at 10.6 GPa at room temperature. Fo=forsterite, Au=gold, Pc=periclase, St=stishovite, wad=wadsleyite.

Figure 2. Representative Raman spectra of H-H vibration mode of hydrogen molecule before heating and after heating at 13.0 GPa (run no.2).

Figure 3. (a) A TEM image of the sample recovered from 15.0 GPa, 1500 K (run no. 4). Right edge of the sample was damaged by a Ga ion beam at FIB. (b) A representative electronic diffraction pattern obtained from the laser heating spot. Fo=forsterite, Au=gold, Pc=periclase, St=stishovite.

Figure 4. A TEM image of the boundary of the laser heating spot and lower temperature region, which has been magnified from Fig 3 (a). Fo=forsterite, Pc=periclase, St=stishovite.

Figure 5. SEM images of the sample recovered to ambient condition (run no. 5). (a) Whole recovered sample in an Re foil gasket. (b) Spherulite of quartz. (c) Columnar and dendritic texture of periclase.

Figure 6. Optical microphotographs of SiO_2-H_2 system (run no. 6). (a) Before heating at

1.7 GPa, (b) After heating at 2.0 GPa, 1700 K. The dashed circle indicates the laser heating spot.

Figure 7. SEM images of the SiO_2-H_2 sample recovered to ambient condition (run no. 6). (a) Etch pits on the surface of quartz crystals. (b) Spherulite texture of quartz.

This is a preprint, the final version is subject to change, of the American Mineralogist (MSA)
Cite as Authors (Year) Title. American Mineralogist, in press.
(DOI will not work until issue is live.) DOI: http://dx.doi.org/10.2138/am.2014.4434

TABLE1 Experimental conditions and run products of Mg_2SiO_4-H_2 system.

Run no.	Starting materials	Laser	Laser absorber	Pressure (GPa) before heating	Pressure (GPa) after heating	Temperature (K)	Analytical methods	Run products
1	Fo-H_2	YAG	Au	11.5	11.8	>1900[a]	XRD (HT), Raman, SEM	Fo, wad, Pc, St
2	Fo-H_2	YAG	Au	11.1	10.6	>2100[a]	XRD (HT), Raman, TEM	Fo, wad, Pc, St
3	Fo-H_2	CO_2	-	11.6	10.0	1600	XRD (RT), Raman, SEM	Fo, Pc, St
4	Fo-H_2	CO_2	Au	15.4	15.0	1500	XRD (RT), Raman, TEM	Fo, Pc, St
5	Fo-H_2	CO_2	-	2.3	2.5	1400	XRD (RT), Raman, SEM	Fo, Pc, Qtz
6	SiO_2-H_2	CO_2	-	1.7	2.0	1700	Raman, SEM	Qtz
7	MgO-H_2	CO_2	-	3.2	3.2	1700	Raman, SEM	Pc

Fo=forsterite, Wad=wadsleyite, Pc=periclase, St=stishovite, Qtz=quartz

XRD (HT) = XRD measurement during heating, XRD (RT) = XRD measurements at room temperature.

[a] maximum temperature of run no. 1 to run no. 2 could not be measured.

This is a preprint, the final version is subject to change, of the American Mineralogist (MSA)
Cite as Authors (Year) Title. American Mineralogist, in press.
(DOI will not work until issue is live.) DOI: http://dx.doi.org/10.2138/am.2014.4434

Figure 1.

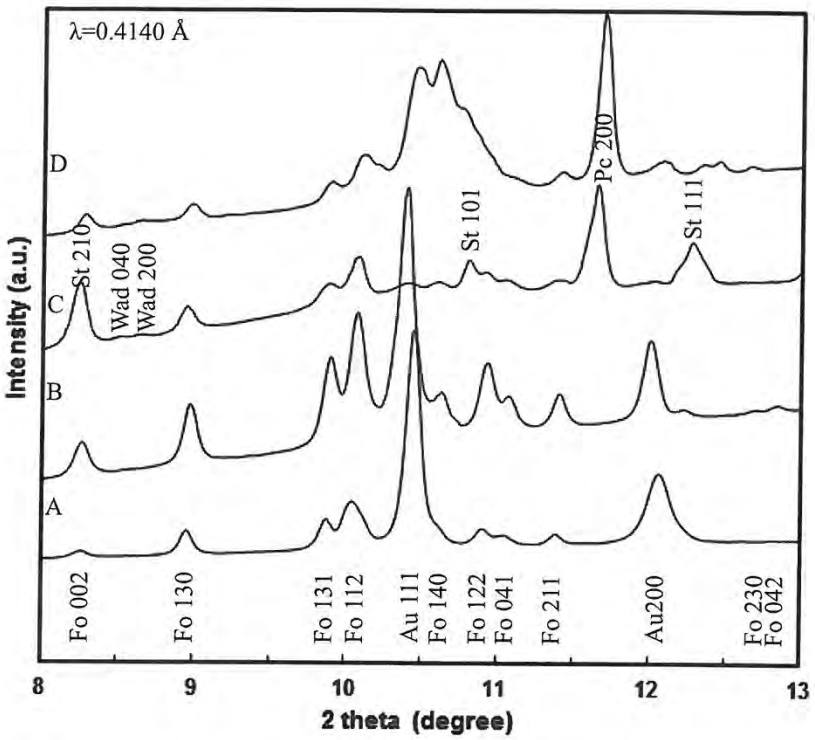

This is a preprint, the final version is subject to change, of the American Mineralogist (MSA)
Cite as Authors (Year) Title. American Mineralogist, in press.
(DOI will not work until issue is live.) DOI: http://dx.doi.org/10.2138/am.2014.4434

Figure 2.

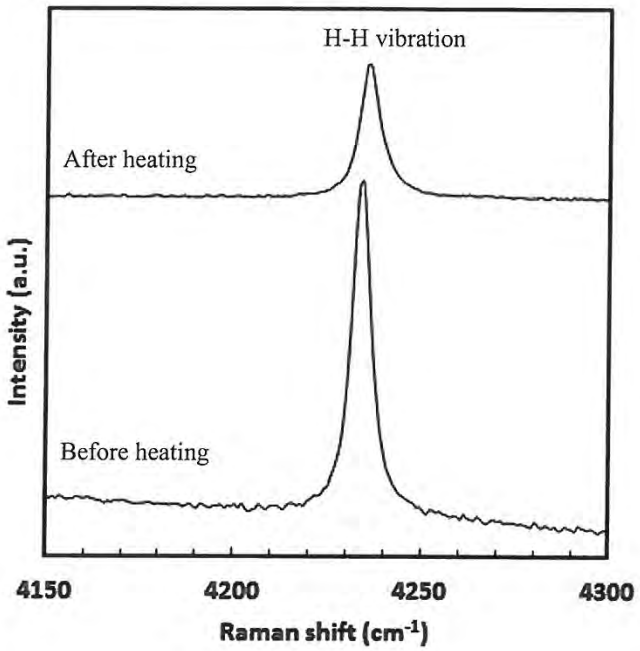

This is a preprint, the final version is subject to change, of the American Mineralogist (MSA)
Cite as Authors (Year) Title. American Mineralogist, in press.
(DOI will not work until issue is live.) DOI: http://dx.doi.org/10.2138/am.2014.4434

Figure 3.

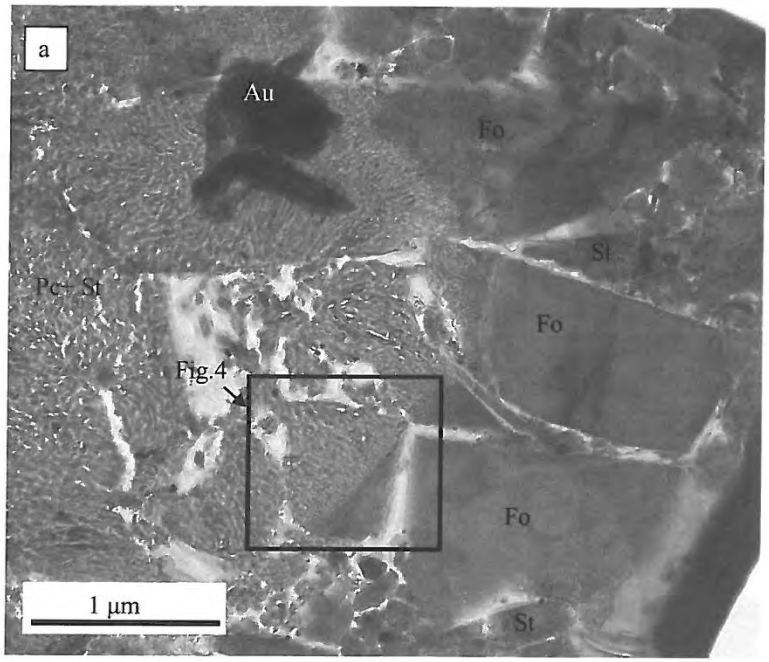

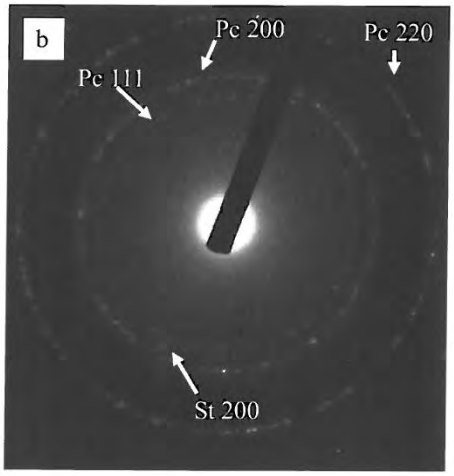

Figure 4.

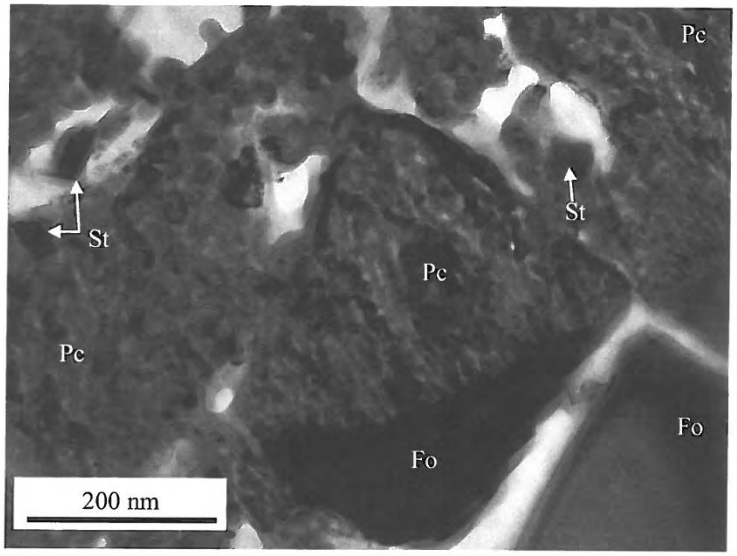

Figure 5.

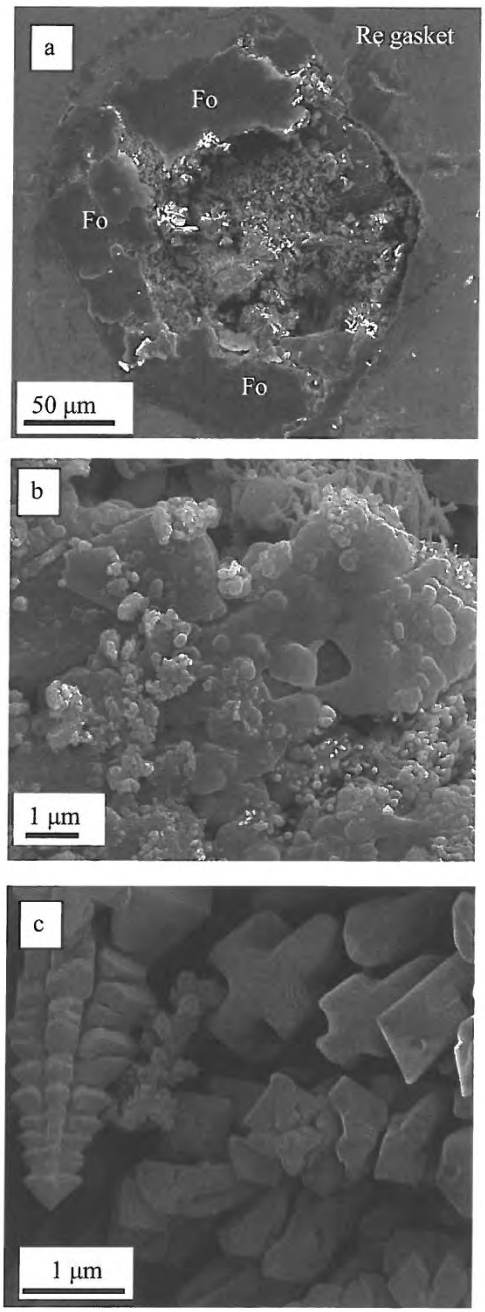

This is a preprint, the final version is subject to change, of the American Mineralogist (MSA)
Cite as Authors (Year) Title. American Mineralogist, in press.
(DOI will not work until issue is live.) DOI: http://dx.doi.org/10.2138/am.2014.4434

Figure 6.

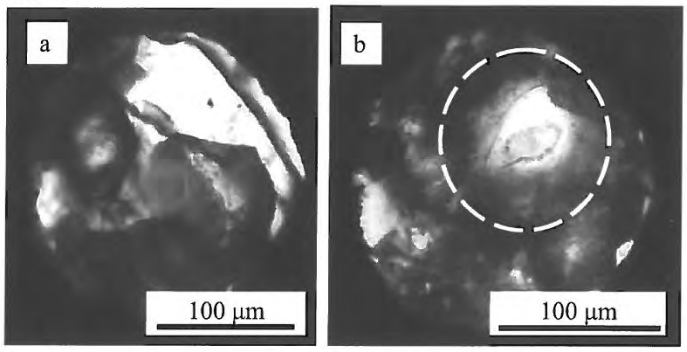

Figure 7.